ResearchGate

See discussions, stats, and author profiles for this publication at: https://www.researchgate.net/publication/228436726

Temperature Dependence of the Free Energy, Enthalpy, and Entropy of P+ QA- Charge Recombination in Rhodobacter s phaeroides R-26 Reaction Centers

ARTICLE *in* THE JOURNAL OF PHYSICAL CHEMISTRY B · AUGUST 2000

Impact Factor: 3.3 · DOI: 10.1021/jp000543v

CITATIONS
34

READS
7

2 AUTHORS, INCLUDING:

Marilyn R Gunner
City College of New York
72 PUBLICATIONS **4,350** CITATIONS

SEE PROFILE

Available from: Marilyn R Gunner
Retrieved on: 25 January 2016

Temperature Dependence of the Free Energy, Enthalpy, and Entropy of $P^+Q_A^-$ Charge Recombination in *Rhodobacter sphaeroides* R-26 Reaction Centers

Qiang Xu and M. R. Gunner*

Department of Physics, Room J419, City College of New York, 138th Street and Convent Avenue, New York, New York 10031

Received: February 10, 2000; In Final Form: May 1, 2000

For reaction centers of photosynthetic bacteria reconstituted with low-potential quinones in the Q_A site, the state $P^+Q_A^-$ formed by light activation decays to the ground state via a thermally activated route through the P^+H^- state. The rate of charge recombination by this thermal pathway is proportional to the equilibrium constant between $P^+Q_A^-$ and P^+H^-. Thus, the free energy difference between $P^+Q_A^-$ and P^+H^- can be determined by measuring the charge recombination rate via the uphill route. The enthalpy and entropy change of the reaction can then be deduced from the temperature dependence of the charge recombination kinetics. The free energy, entropy, and enthalpy changes between $P^+Q_A^-$ and P^+H^- were determined at temperatures from 40 to 318 K for several low-potential quinones. From 200 K to room temperature, $\Delta H° \approx \Delta G°$, so the entropy changes are small. However, in the temperature range 80−200 K, a significant entropy change is observed, and the free energy becomes strongly temperature-dependent. The newly formed $P^+Q_A^-$ state lives for milliseconds. On this time scale at low temperature, the $P^+Q_A^-$ state appears to be trapped prior to charge recombination in a state ∼200 meV (10 K) higher in free energy than the relaxed form found at room temperature.

Introduction

The bacterial photosynthetic reaction center (RC) is the intrinsic membrane protein that facilitates the conversion of light energy to chemical energy. Upon absorption of a photon, charge separation is achieved by a series of electron transfers between the cofactors bound to the protein. The crystal structure and the electron-transfer sequence of RCs from several species of bacteria have been well characterized (for reviews, see refs 1−3). Electron transfer in this protein proceeds through a quantum tunneling mechanism. This protein has proved to be an ideal model system for studying the basic chemistry of electron transfer in biology and chemistry.[4,5] In addition to the advantages of having a well-defined configuration of electron donors and acceptors, sophisticated methods are available to change the driving force of the reaction and to manipulate the local protein environment of the cofactors.[6−9] In addition, most of the electron-transfer steps in this protein are able to proceed at cryogenic temperature, providing unique advantages for the study of protein dynamics.[10−14]

Charge separation in reaction centers starts with a very fast picosecond electron transfer from the primary electron donor P, a dimer of bacteriochlorophyll, to the bacteriopheophytin H in the active L branch of the protein, followed by a slower reduction (∼200 ps) of the primary quinone Q_A. When the secondary quinone Q_B is absent, the resultant charges on P^+ and Q_A^- recombine to return the system to the ground state (Figure 1). Following the electron transfer from P* to H, the system can return to the ground state in a reaction that competes with the forward electron transfer to Q_A. Because of spin rephasing in the P^+H^- state, charge recombination yields the triplet ^3P as well as the singlet P. ^3P returns to ground state through relatively slow intersystem crossing.[15,16]

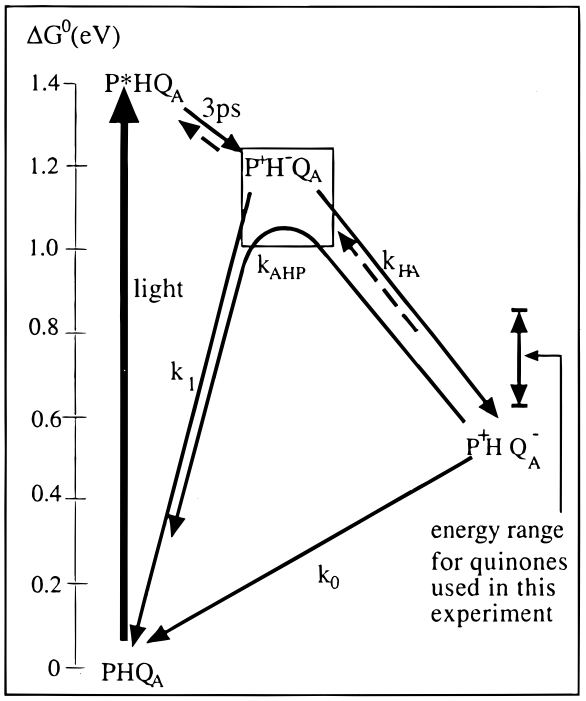

Figure 1. Electron-transfer pathway and free energy level in *Rb. spharoides* RCs. The free energy level of the $P^+HQ_A^-$ state is shown for the native ubiquinone. The energy range for the substituted low-potential quinones used as Q_A in the experiment is also shown. The uncertainty of the P^+H^- free energy level is indicated by the box (see discussion). With native RCs at room temperature, $k_1 = 7.7 \times 10^7\ s^{-1}$ and is assumed to be independent of quinone at the Q_A site, $k_{HA} = 5 \times 10^9\ s^{-1}$, and $k_0 = 9.3\ s^{-1}$.

Several different methods have been applied to reaction centers from *Rhodobacter sphaeroides* strain R-26 to measure the free energy, enthalpy, and entropy of different reactions.

* Author to whom correspondence should be addressed. Telephone: 212-650-5557. Fax: 212-650-6940. E-mail: gunner@sci.ccny.cuny.edu.

10.1021/jp000543v CCC: $19.00 © 2000 American Chemical Society
Published on Web 07/21/2000

The energy level of $P^+Q_A^-$ relative to other states has been determined in several ways. During the slow $P^+Q_A^-$ charge recombination process, $P^+Q_A^-$ and P* are in pseudo-equilibrium. The fraction of the population in which electrons return to the donor to reform the P* state can be determined from the integrated amplitude of delayed fluorescence from P*. The ratio of P* and $P^+Q_A^-$ in pseudo-equilibrium provides the free energy difference between the two redox states**.** The enthalpy and entropy changes of the reaction can then be deduced from the temperature dependence of the delayed fluorescence.[17,18] A second, photoacoustic, method measures the enthalpy change of the reaction directly from the heat released during the electron transfer from P* to $P^+Q_A^-$. Given the reaction free energy obtained by other methods, the entropy change can be found.[19−21]

A third method for determining in situ thermodynamic parameters utilizes the fact that the $P^+Q_A^-$ charge recombination can proceed through two pathways. One is by direct electron tunneling from Q_A^- to P^+. In the other, $P^+Q_A^-$ equilibrates with a higher-energy state, most likely P^+H^-, which then decays to the ground state.[18,22−24] The rate of charge recombination by this thermal pathway is proportional to the equilibrium constant between $P^+Q_A^-$ and P^+H^- and to the rate of charge recombination from P^+H^-. Thus, by measuring the charge recombination rate via this uphill route, the free energy difference between $P^+Q_A^-$ and P^+H^- can be determined using the known P^+H^- decay rate. With the native ubiquinone-10 as Q_A, the activated state is 520 meV higher in energy than the $P^+Q_A^-$ state, so the contribution of the uphill route to charge recombination is negligible compared to that of the direct route in the ambient temperature range. However, the ubiquinone in the Q_A site can be replaced with other quinones, a technique that allows the free energy change of reaction involving Q_A to be modified.[18,22,34] With substituted quinones with in situ redox potentials more than 100 meV lower than that of ubiquinone, the rate via this thermal route is comparable to or even much faster than the direct route.

The energy of $P^+Q_A^-$ with different quinones as Q_A measured by the rate of the thermal back reaction is consistent with that determined by the delayed fluorescence measurement[18] (Figure 2) and with values measured by $P^+Q_B^-$ charge recombination through $P^+Q_A^-$ as an intermediate state.[9,25] Thermal back reaction measurements have been applied to reaction centers with a series of low-potential quinones[11,18] and several nonquinone compounds[26] as Q_A. This activated reaction has been used to measure the effects of pH,[27,28] external electrical field,[6,13] and mutation[25] on the in-situ quinone redox potential.

Measurement of the temperature dependence of the uphill charge recombination rate provides the enthalpy change of this reaction.[18,26,28] The reaction free energy, entropy, and enthalpy influence the electron-transfer rate and the portion of the photon's energy that is stored. A significant entropy change could indicate that conformational changes or the binding or release of waters or ions are coupled to the electron-transfer reaction. In the absence of direct measurements, most theoretical treatments of electron transfer in reaction centers assume that the entropy change is negligible.[4,5,29]

The changes in entropy and enthalpy of several reactions involving Q_A have been investigated near room temperature. There are indications from delayed fluorescence that the change in entropy for the charge separation forming $P^+Q_A^-$ from P^*Q_A is small.[17,18] Although several photoacoustic measurements also found that $\Delta H°$ is close to $\Delta G°$ for this reaction,[19,20] recent photoacoustic measurements indicate, instead, that there may be a significant entropy change for the same process. A $T\Delta S°$ value of 420 meV (298 K) was found for native RCs for which $\Delta G°$ is −860 meV.[21]

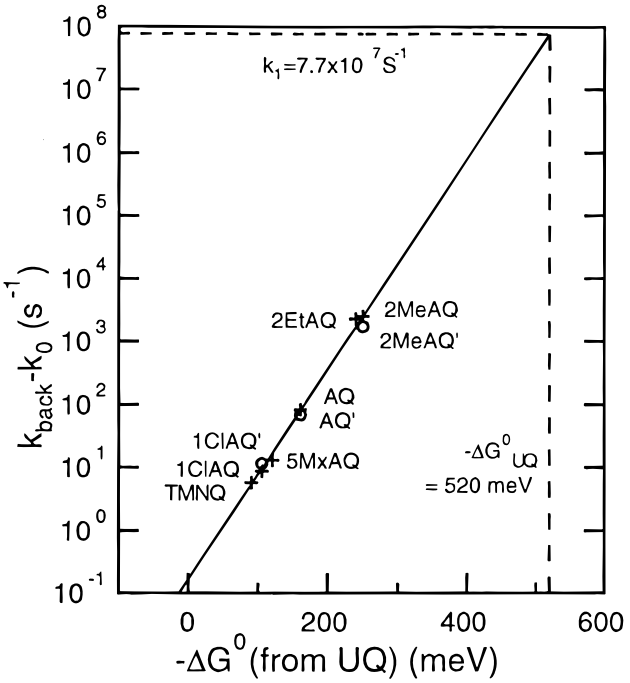

Figure 2. Relation between the $P^+Q_A^-$ charge recombination rate and the in situ free energy measured by delayed fluorescence.[18] +, charge recombination rates taken from ref 41; ○, values measured here. The line through the data was drawn so that the rate increases by a factor of 10 for each 60 meV increase in the energy of $P^+Q_A^-$, as predicted if the reaction mechanism involves equilibration of $P^+Q_A^-$ with a higher-energy state. Assuming that this state decays at a rate of 7.7×10^7 s^{-1}, as expected for P^+H^-, the intermediate is 520 meV above $P^+Q_A^-$ when Q_A is UQ. TMNQ, 2,3,5-trimethylnaphthoquinone; 2EtAQ, 2-ethylanthraquinone; and 5MxAQ, 5-methoxyanthraquinone. See Experimental Section for other abbreviations.

The temperature dependence of the $P^+Q_A^-$ thermal charge recombination rate has been measured with several different quinones as Q_A.[11,28] With anthraquinone as Q_A, $\Delta H°$ changes between $P^+Q_A^-$ and P^+H^- by ∼400 meV, while $T\Delta S°$ is ∼40 meV. The temperature dependence of the charge recombination kinetics for several nonquinone compounds that are functional in the Q_A site also showed enthalpy changes close to the reaction free energy change.[26] Measurements in reaction centers from *Rhodopseudomonas viridis* also showed also showed small values for $\Delta S°$.[23,30]

The ability to measure thermodynamic parameters over a wide temperature range allows the comparison of the protein above and below the solvent freezing and glass transition temperatures. This can provide additional information on the protein dynamics. The region around 200 K is of particular interest.[31] Temperature-dependent transitions of the equilibrium dynamical fluctuations in several proteins have been observed at 200−220 K.[32] The solvent glass transition (Tg) is also found in this region. Tg is about 180 K for 3:1 glycerol−water mixtures, a common solvent for low-temperature measurements with protein, which may influence the measured protein reaction kinetics.[33] Previous studies of the thermal back-reaction kinetics with nonquinone compounds and in RCs from *Rps. viridis* have been extended to cryogenic temperatures. However, the temperature range for these earlier measurements was still quite restricted. Either the indirect route of $P^+Q_A^-$ charge recombination was frozen out above 200 K[23,26,30] or measurements were only made at temperatures well below 200 K.[26]

Previous studies of reaction centers with the native ubiquinone-10 as Q_A showed that the exothermic, direct tunneling $P^+Q_A^-$ charge recombination rate undergoes an increase of about 4-fold over a relatively narrow temperature range around 200 K.[14] It has been suggested that this arises from changes in the $P^+Q_A^-$ energy level due to changes in the distribution of accessible protein conformations with temperature. Further evidence for changes in the temperature region was also found in studies of the same reaction in mutants with a modified P/P^+ midpoint potential. It was shown that the sum of the electron-transfer reorganization energy and the reaction free energy decreases by about 280 meV from 293 to 10 K, with the sharpest decline near 200 K.[34]

The work presented here reports a systematic study of the temperature dependence for the $P^+Q_A^-$ thermal charge recombination kinetics at temperatures from 40 to 318 K. Eight low-potential anthraquinones and one naphthoquinone were substituted into the Q_A site. These quinones vary the free energy change of the reaction by about 200 meV. The results clarify some of the discrepancies between different previous measurements and extend the measurement to cover a wider temperature range. Additional evidence is found for a change in protein relaxation for the formation of the $P^+Q_A^-$ state in the temperature region near 200 K.

Experimental Section

Reaction centers of *Rb. sphaeroides* strain R-26 were isolated following established procedures using lauryldimethylamine-*N*-oxide (LDAO) extraction and were purified using ammonium sulfate and DEAE (diethylaminoethyl) chromatography.[35] The native ubiquinones in the Q_A and Q_B sites were extracted with 4% LDAO and 10 mM orthophenathroline using the method of Okamura[36] with minor modifications.[18] The typical residual quinone after the treatment is $Q_A \leq 5\%$ and $Q_B = 0\%$. In the final assay mixture, the residual LDAO concentration from the RC stock solution is less than 0.025%. For Q_A reconstitution, quinones were first dissolved in alcohol, and then added to the sample at the desired concentration. The buffer used was 10 mM Tris with 2.5 mM KCl (pH = 8.0). The following eight anthraquinones and one naphthoqinone were used: 1-chloroanthraquinone (1-Cl-AQ), 2-chloroanthraquinone (2-Cl-AQ), 2-aminonaphthoquinone (2-Am-NQ), anthraquinone (AQ), 2-methylanthraquinone (2-Me-AQ), 1-aminoathraquinone (1-Am-AQ), 2,3-dimethylanthraquinone (2,3-dM-AQ), 2,7-dimethylanthraquinone (2,7-dM-AQ), and 1,3-dimethylanthraquinone (1,3-dM-AQ). 2,7-dM-AQ was synthesized in the laboratory of Dr. J. Malcolm Bruce (University of Manchester); the other quinones were purchased from Fluka (AQ and 2-Am-AQ) and Aldrich (all others).

Charge recombination kinetics were observed in a flash spectrometer of local design. The electron-transfer reaction was initiated by a 10-μs xenon flash. The changing redox state of the electron donor P was followed by monitoring the absorption change at 430 nm. The transmitted light was collected by a photomultiplier tube (Thorn EMI9798QB). The signal was filtered and amplified before being sent to a LeCroy digital oscilloscope (model 9310M, 300 MHz).

The temperature dependence of the charge recombination reaction was measured in the range of 5−45 °C for all nine quinones substituted into the Q_A site. The reaction center concentration was 300−400 nM. The temperature was controlled by using a jacketed cuvette with a circulating waterbath (Fisher model 9101). A thermocouple monitors the temperature change with an accuracy of 0.1 °C. Measurement starts ~5 min after the sample reaches the preset temperature. For each measurement, 10−15 traces were averaged.

For reaction centers with 2-Cl-AQ, 2-Me-AQ, and 2,3-dM-AQ as Q_A, the $P^+Q_A^-$ charge recombination reaction was monitored at temperatures from 40 to 300 K. The temperature was controlled by a closed-cycle helium cryostat system (APD Cryogenics Inc., model CSW202A) with a programmable temperature controller. The temperature resolution is 0.1 K, and the controllability is ±0.4 K. The samples used for the low-temperature experiment were obtained by mixing the reaction centers in Tris buffer with two volumes of glycerol. The final reaction center concentration is 3−4 μM. The optical cell has a light path of 1 mm. The actinic and measuring light, which are perpendicular to each other, meet with an incident angle of 45° at the sample.

The observed kinetics were analyzed by both one- and two-exponential decays plus a constant using a nonlinear least-squares fitting program using the Levenberg−Marquardt algorithm (Igor Pro from WaveMetrics). For 2-Me-AQ and 2,3-dM-AQ at low temperature, an extra exponential function is needed to fit a fast phase that decays at a rate of about 5000 s^{-1}. This phase arises because of formation of the triplet state of the bacteriochlorophyll dimer (^3P) at low temperature.[37]

The observed reaction kinetics monitor the charge recombination in the $P^+Q_A^-$ state, which proceeds through a thermally activated pathway via P^+H^-, in addition to the direct tunneling rate (Figure 1). Because the uphill rate monitors the equilibrium constant, the temperature dependence of the kinetics can provide the enthalpy and entropy differences between $P^+Q_A^-$ and P^+H^-. The charge recombination rate can be written as

$$k = k_0 + k_1 \exp(-\Delta G^\circ/k_B T) = k_0 + k_1 \exp(\Delta S^\circ/k_B) \exp(-\Delta H^\circ/k_B T) \quad (1)$$

where k_0 is the rate by the direct electron tunneling route, which is relatively temperature independent.[10,11] k_1 is the quinone-independent decay rate from P^+H^- for reforming the ground state, k_B is the Boltzman constant, and T is temperature. ΔG°, ΔH°, and ΔS° are the standard free energy, enthalpy, and entropy changes between $P^+Q_A^-$ and P^+H^-. The thermodynamic parameters are obtained from the van't Hoff plot of $\log(k - k_0)$ vs $1/T$.

$$\log(k - k_0) = \log k_1 + (\Delta S^0/2.3k_B) - (\Delta H^0/2.3k_B T) \quad (2)$$

Results

Analysis of the Charge Recombination Kinetics. The temperature dependence of the $P^+Q_A^-$ charge recombination kinetics was measured at temperatures from 40 to 318 K in reaction centers substituted with different low-potential quinones. The exact value of the rate is sensitive to the fitting procedure. The charge recombination kinetics were fit using single, double, and distributed rate functions. With a double exponential, the fast rate (k_f) is 2−3 times the slower rate (k_s) in the ambient temperature range for all Q_A's with in situ midpoint potentials more positive than that of 1-Am-AQ (−285 meV relative to UQ_{10}). As the Q_A midpoint is lowered, the rate becomes substantially faster (Figure 2). The limited resolution of the measurements provides enough data for only single-exponential fits. For the higher-potential Q_A's, the double exponential fits the kinetic data with no systematic error, whereas the single exponential fit underestimates the amplitude at early times (See Figure 3). This has been observed previously.[28,30,38] The different rates have been attributed to two populations of reaction centers with different protonation states

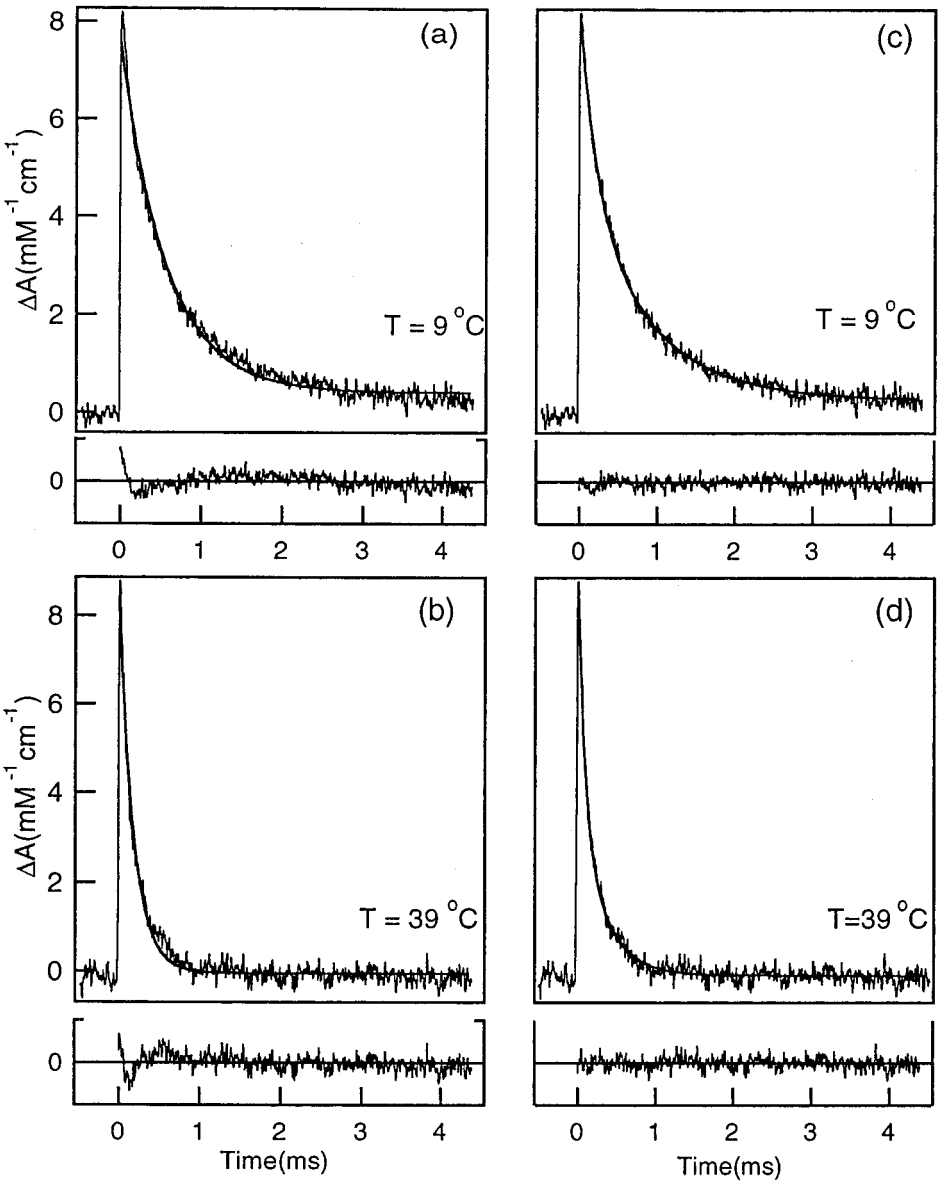

Figure 3. Flash-induced absorption change for RCs with 2-Me-AQ as Q_A. The single- (a and b) and double- (c and d) exponential fits to the kinetics at two different temperatures are shown. The residual error is also shown. pH = 8.0, [RC] = 400 nM, [2-Me-AQ] = 4 μM. k_{single} is the rate obtained from the single-exponential fit while k_f and k_s are the faster and slower components of the double-exponential fit. The fit parameters are the following: at $T = 9$ °C, $k_{single} = 1.8 \times 10^3$ s^{-1}, $k_f = 1.2 \times 10^3$ s^{-1} (46% of total amplitude), and $k_s = 4.6 \times 10^3$ s^{-1} (54%); and at $T = 39$ °C, $k_{single} = 5.4 \times 10^3$ s^{-1}, $k_f = 3.2 \times 10^3$ s^{-1} (55%), and $k_s = 1.2 \times 10^4$ s^{-1} (45%). The constant in the single-exponential fit is less than 5% of the total amplitude in both cases.

of residues close to the Q_A binding site.[28] Because the fast and slow phases are not very different, the parameters obtained for the two rates have larger uncertainty than that of the single-exponential fit. The rates of charge recombination in RCs with 2-Me-AQ as Q_A in aqueous solution are plotted in Figure 4. As will be shown later, the values of $\Delta G°$ and $\Delta H°$ are only weakly dependent on the fitting procedure. Therefore, the simplest single-exponential analysis will be used.

More complicated fitting schemes using distributed rates have been suggested by Kleinfeld et al.[10] and McMahon et al.[14] for analysis of low-temperature kinetics, which assumes a distribution of conformational states. The result from the single-rate method can be regarded as the weighted-average value of the distribution.[39] The data obtained here can be fit as well by two exponential functions as by a model with a distribution of rate constants (not shown).

An additional complication is found at low temperature for the low-potential Q_A's. In RCs with 2-Me-AQ and 2,3-dM-AQ as Q_A, an extra fast phase with a rate of approximately 5000 s^{-1} was observed below 200 and 220 K, respectively. This phase can be attributed to the decay of the triplet state ^3P.[37,40] As expected, a phase with the same rate constant but larger amplitude is seen in reaction centers with no Q_A, but is not seen in reaction centers containing the native ubiquinone-10. The rate of this phase is fixed in the analysis of the reaction kinetics using the value measured in reaction centers with no Q_A.

The rates obtained by single-exponential fits for reaction centers with several different low-potential quinones as Q_A in the temperature range 220−318 K are shown in Figure 5. The rate varies with in situ E_m, as discussed in the Experimental Section. It accelerates with increasing temperature as expected if $\Delta H°$ is significant. Figure 6 shows the temperature dependence of the reaction at temperatures between 40 and 300 K for reaction centers with 2-Me-AQ, 2,3-dM-AQ and 2-Cl-AQ as Q_A.

Aqueous buffer was used for measurement in the ambient temperature range, whereas in the low-temperature experiments,

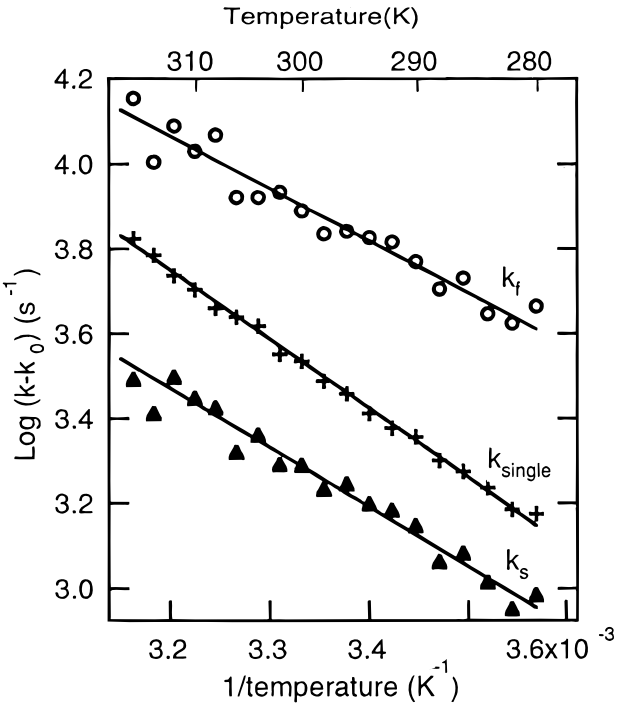

Figure 4. van't Hoff plot for the single-exponential fit and for the two phases (k_f, k_s) of a double-exponential fit of the charge recombination for 2-Me-AQ in the ambient temperature range. Fitting parameters are given in Table 1.

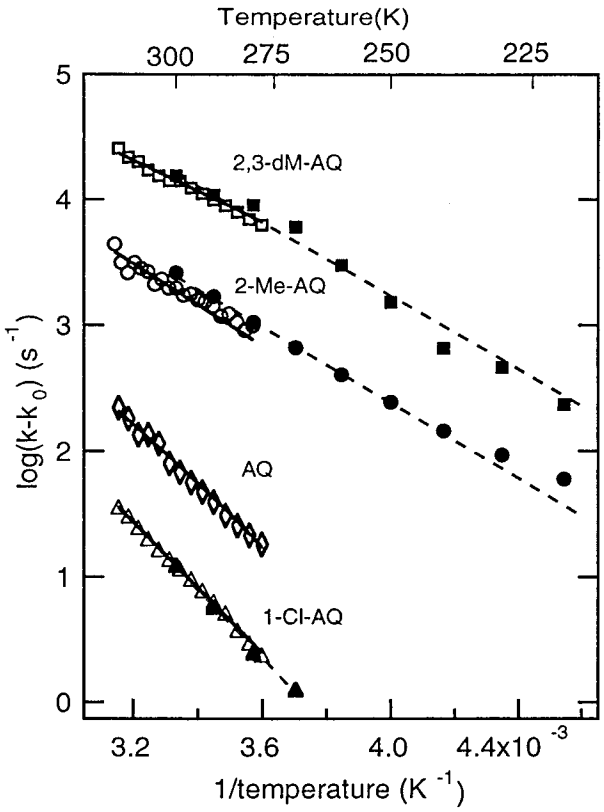

Figure 5. Temperature dependence of the $P^+Q_A^-$ charge recombination rates for reaction centers with four different Q_A's. The rates are obtained from single-exponential fits to the kinetic data. Solid symbols represent values measured in the 210−300 K region (with 67% glycerol), and open symbols represent values measured between 278 and 318 K. ■ and □, 2,3-dM-AQ; ●and ○, 2-Me-AQ; ◊, AQ; and ▲ and △, 1-Cl-AQ. The lines shown are fits to eq 2. Fitting parameters are given in Table 2.

67% glycerol solution was used. The $P^+Q_A^-$ charge recombination rate in glycerol solution is very close to the rate in aqueous solution at the same temperature (Figure 5). This differs from previous results with *Rps. viridis* reaction centers, where the rate was found to decrease when glycerol was added.[23]

Choice of k_0 and k_1. The free energy, enthalpy, and entropy changes in going from $P^+Q_A^-$ to P^+H^- can be obtained using eq 2, given the $P^+Q_A^-$ charge recombination rate through the direct electron tunneling route, k_0, and the charge recombination rate from P^+H^-, k_1. The direct electron tunneling rate from Q_A^- to P^+, k_0, is only weakly temperature dependent.[34,41] Thus, for each Q_A, the low-temperature value (∼35 K) was used for k_0 at all temperatures. This rate was either measured here or taken from earlier studies.[41] For most of the Q_A's used here, the charge recombination rate is over 100 s^{-1} in the ambient temperature range. This is much larger than k_0, which is less than 30 s^{-1}, so the fitting process is not sensitive to errors in k_0. However, for 1-Cl-AQ and 2-Cl-AQ, whose charge recombination rates (∼20 s^{-1}) are of the same magnitude as their k_0's (∼10 s^{-1}), the fitting is sensitive to the choice of k_0. For these relatively high potential Q_A's, increasing k_0 by 1 s^{-1} increases the $T\Delta S°$ estimate by 50 meV. Given k_0, the temperature dependence of the measured charge recombination rate can be fit using eq 2. The slope of the resultant line gives the standard enthalpy change between $P^+Q_A^-$ and P^+H^- (Figure 4).

The charge recombination rate was measured down to 275 K with all nine Q_A's. In this temperature range, there is a clear, simple linear dependence between the rate and $1/T$. Measurements of the rate were continued to 40 K for reaction centers with three of the Q_A's. Above ∼210 K, the charge recombination rate decreases with the temperature as predicted by eq 2 (Figure 5), with essentially the same slope as found in the aqueous sample at room temperature. The entropy change is quite small in this temperature region. However, below ∼210 K, the rate decreases much more slowly as the temperature decreases. The temperature dependence at temperatures between 80 and 210 K suggests the reaction has a much smaller enthalpy (Figure 6). For these two Q_A's, $\Delta H°$ is close to 300 meV above 200 K and only 30 meV below the transition temperature (Table 3). Below 210 K, the kinetics do deviate more from a simple exponential decay. However, a double-exponential function still fits the data well. The slow and fast phases exhibit a similar temperature dependence and therefore have similar enthalpies (data not shown).

The kinetics for reaction centers with 2,3-dM-AQ were also measured in 33% glycerol buffer (Figure 6b). As the temperature is lowered from room temperature the reaction rate and the enthalpy are independent of the solvent. However, the temperature of transition to a smaller enthalpy reaction occurs about 15 K higher in the low-glycerol sample. Thus, this transition seems to relate to some property of the solvent. Below the transition temperature, the temperature dependence of the rate is the same in both low- and high-glycerol solvents. Thus, the reaction enthalpy is unaffected by this change in solvent. However, the reaction $\Delta G°$ is dependent on the glycerol concentration, as seen by the faster back-reaction rate with the lesser glycerol concentration. The solvent changes the reaction $\Delta S°$.

To determine the reaction free energy and entropy from the observed $P^+Q_A^-$ decay kinetics, the charge recombination rate of P^+H^-, k_1, is needed. This decay rate has been previously established to be $\sim 5-8 \times 10^7$ s^{-1}.[37,40] For the calculation reported here, k_1 is taken to be 7.7×10^7 s^{-1}. Different values have been used when the triplet decay pathway was taken into consideration.[23,42] However, as will be discussed later, the triplet

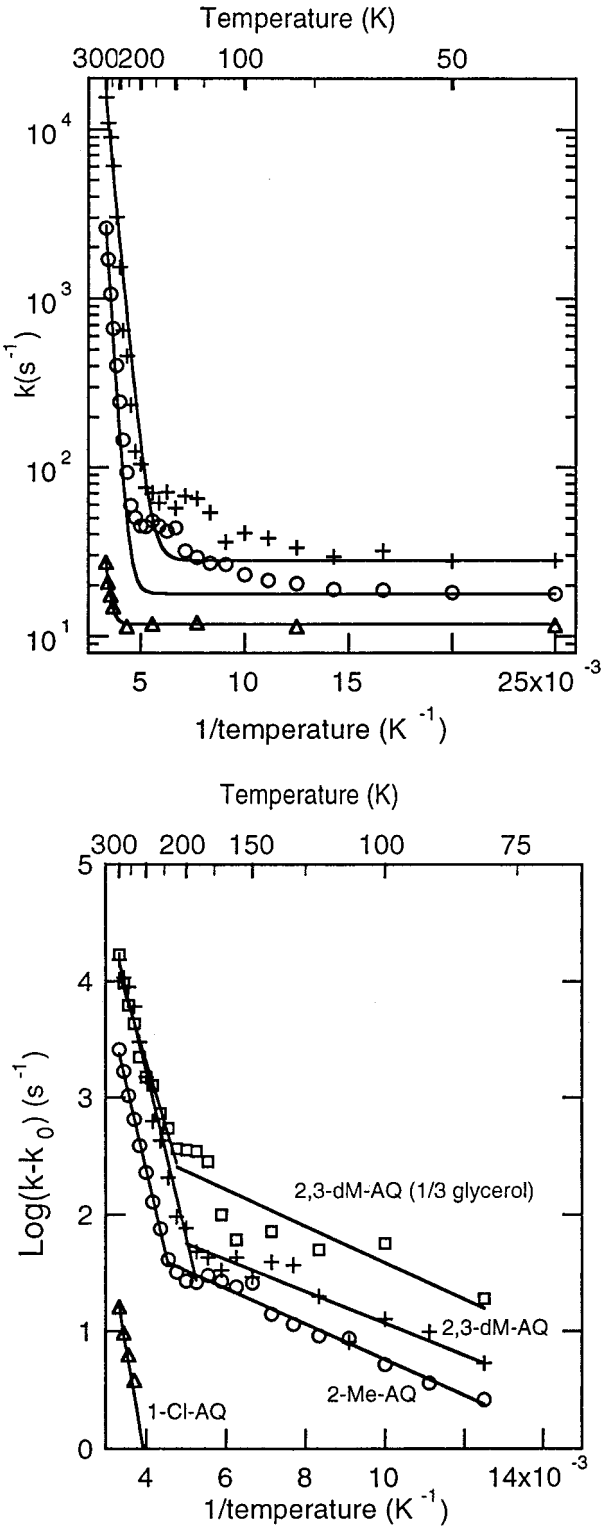

Figure 6. Temperature dependence of the $P^+Q_A^-$ charge recombination rate (single-exponential fit) for three different quinones as Q_A (40−300K). With 67% glycerol, +, 2,3-dM-AQ; ○, 2-Me-AQ; and ▲, 1-Cl-AQ; and with 33% glycerol, ◇, 2,3-dM-AQ (b only). Fitting parameters given in Table 3. (a) Fit to eq 1. (b) Data fit with contribution of direct tunneling pathway (k_0) subtracted and eq 2 fit independently above and below transition temperature.

pathway seems to be separate from the charge recombination pathway found in these reaction centers. k_1 has a weak temperature dependence.[37,40] The rate increases approximately 20% at temperatures from 5 to 45 °C, causing a −30 meV correction of the enthalpy measured in this temperature range for all the quinones. This correction is smaller (approximately −10 meV) for the enthalpy measurements over the larger temperature range. The reported enthalpy was corrected for the temperature dependence of k_1.

TABLE 1: Free Energy, Enthalpy, and Entropy Changse from $P^+Q_A^-$ to P^+H^- in RCs with 2-Me-AQ as Q_A, Using Different Fitting Procedures

	rate[a]		$\Delta G°$ [b] (meV) (298 K)	$\Delta H°$ [b] (meV)	$T\Delta S°$ [b] (meV) (298 K)
278−318 K	single		265 ± 7	326 ± 5	61 ± 5
	double	fast	240 ± 23	240 ± 16	0 ± 16
		slow	273 ± 26	273 ± 18	−3 ± 19
210−300 K	single		264 ± 17	297 ± 16	33 ± 5
	double	fast	251 ± 85	277 ± 76	26 ± 40
		slow	280 ± 53	305 ± 45	25 ± 28

[a] Single: Charge recombination fit with a single exponential. Double: fast and slow phases of the two exponential analysis. [b] The error quoted here is the standard deviation of the fitting to the van't Hoff plot.

Entropy, Enthalpy, and Free Energy. The free energy, enthalpy, and entropy changes for reaction centers with 2-Me-AQ as Q_A are listed in Table 1. These values compare measurements in the ambient temperature range (278−318 K) and in 67% glycerol at temperatures between 220 and 300 K. Remarkably, the results show that the reaction entropy and enthalpy is temperature-independent down to 220 K. The enthalpy change is the dominating term, being close to the reaction free energy, and so the entropy change is small. Thus, the free energy is nearly temperature-independent. The $\Delta G°$ value obtained for the single-exponential fit is 265 meV (298 K). This is in good agreement with previous measurement of 270 meV.[12,18] The free energy difference between the fast and slow phases is about 30 meV (298 K), which reflects the approximately 3-fold difference in the two rate constants.

The parameters from the single-exponential fit above the transition temperatures for reaction centers with nine different Q_A's are listed in Table 2. The measured entropy and enthalpy change vs the free energy change are plotted in Figure 7. The enthalpy change is slightly larger than the free energy change, and the difference becomes smaller when $\Delta G°$ decreases. On average, $\Delta H°$ is within 10% of $\Delta G°$. AQ has the largest absolute entropy change, $T\Delta S° = 100$ meV, whereas in 1-Am-AQ, the entropy change is the largest fraction of the reaction free energy change. The entropy change is never more than 25% of the reaction $\Delta G°$.

The reaction enthalpy, entropy, and free energy were determined at temperatures below 210 K using the same thermal back-reaction model and the same k_1 value (Table 3). The enthalpy drops by about 250 meV below the transition temperature, and the entropic contribution to the free energy increases by the same amount. Now, the free energy change decreases with temperature.

One possible source of error in the derivation of the thermodynamic parameters is the use of a constant value for k_0, especially at temperatures below 210 K. Previous studies[34,41] show that k_0 increases by 50−100% from 210 to 90 K in wild-type RCs and in mutants with different P/P^+ midpoint potentials, which is in the opposite direction of the rate change observed here. The use of a constant value for k_0 will cause the enthalpy of the reaction to be underestimated, but it is not nearly enough to explain the difference in the enthalpy change above and below the transition temperature. If k_0 is assumed to double over this temperature range in RCs with substituted quinones, the correction to the enthalpy data derived is less than 3 meV, within the error of the measurement.

TABLE 2: Free Energy, Enthalpy, and Entropy Changes from $P^+Q_A^-$ to P^+H^- for RCs with Nine Different Quinones as Q_A[a]

			278−318 K			210−300 K		
		k_0 (s^{-1})	$\Delta G°$ (meV) (298 K)	$\Delta H°$ (meV)	$T\Delta S°$ (meV) (298 K)	$\Delta G°$ (meV) (298 K)	$\Delta H°$ (meV)	$T\Delta S°$ (meV) (298 K)
1	2-Cl-AQ	12.2	410	460	50			
2	1-Cl-AQ	10.2	391	425	34	402	420	18
3	2-Am−NQ	10.0	364	400	20			
4	AQ	7.4	330	430	100			
5	2-Me-AQ	19.7	265	326	61	264	297	33
6	1-Am-AQ	6.8	234	306	72			
7	1,3-dM-AQ	20.0	221	252	31			
8	2,3-dM-AQ	27.7	219	244	25	200	282	82
9	2,7-dM-AQ	20.9	203	228	25			

[a] The kinetics were fit using a single-exponential plus a constant. The uncertainty of the thermodynamic parameters is less than 25 meV. Measurements between 278 and 318 K use aqueous buffer (Tris pH = 8.0), while those between 210 and 300 K use a 2:1 glycerol−water mixture as the solvent.

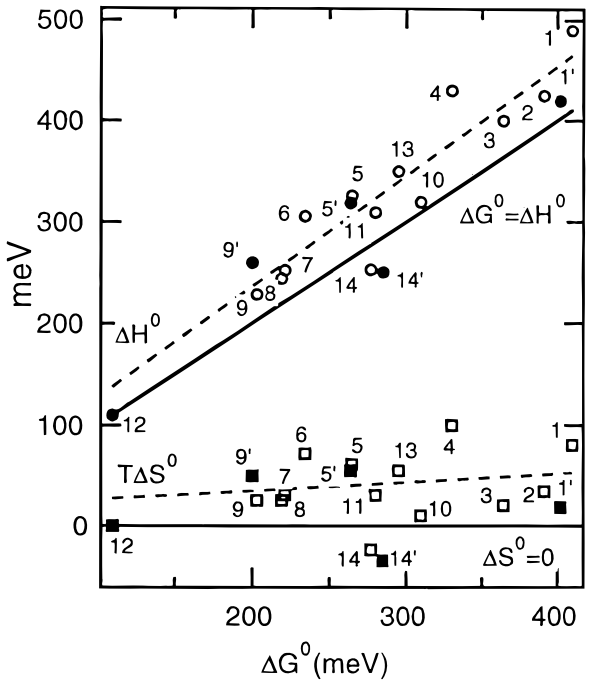

Figure 7. Enthalpy and entropy changes vs free energy change for the reaction from $P^+Q_A^-$ to P^+H^- with eight anthraquinones and one naphthoquinone as Q_A. The lines through $\Delta H°$ and $T\Delta S°$ have slopes of 1.1 and 0.1, respectively. A line with $\Delta G° = \Delta H°$ is also shown. Identity of each reaction center: 1−9 refer to the data in Table 2 measured between 278 and 318 K. The primed labels (1′, 5′, 9′, and 14′) refer to data measured between 210 and 300K. 10−12 refer to data with nonquinones substituted for Q_A from ref 26 with 10, 1-nitroso-2-hydroxynaphthalene; 11, 2,4,7-trinitro-6-fluorenone; and 12, 1,2,3,4-tetrafluoro-9-fluorenone. 10 and 11 were measured between 200 and 300 K; 12 was measured below 150 K. 13 is for AQ as Q_A from ref 28. 14 is for *Rps. viridis* reaction centers with the native menaquinone as Q_A measured between 274 and 308 K.[23]

Discussion

The temperature dependence of the $P^+Q_A^-$ charge recombination kinetics was measured at temperatures from 40 to 318 K for reaction centers with low-potential quinones substituted in the Q_A site. With these Q_A's, the reaction occurs via a preequilibrium with the P^+H^- state.[22] Thus, the reaction kinetics provide a simple measurement of the in situ thermodynamics for the electron transfer from Q_A^- to H. The use of these different Q_A's allows the reaction $\Delta G°$ to be varied over a range of ∼200 meV. In the native RCs with ubiquinone as Q_A, the contribution of the uphill pathway is negligible. Here charge recombination proceeds mainly through direct tunneling from Q_A^- to P. This reaction is close to temperature-independent; therefore, it provides little information about reaction thermodynamics.[11,13] The temperature at which the thermal route freezes out and the direct tunneling rate becomes the dominant pathway decreases as the quinone midpoint potential is lowered.[24]

TABLE 3: Comparison of Free Energy, Enthalpy, and Entropy Changes from $P^+Q_A^-$ to P^+H^- Above and Below the Transition Temperature[a]

	$\Delta G°$ (meV) (298 K)	$\Delta H°$ (meV)	$T\Delta S°$ (meV) (298 K)
	$P^+Q_A^- \rightarrow P^+H^-$		
2-Me-AQ[b]	264	297	33
2-Me-AQ[c]	350	30	−320
2,3-dM-AQ[b]	200	282	82
2,3-dM-AQ[c]	330	30	−300
	$P^+Q_A^- \rightarrow P*$		
2,3-dM-AQ[d]	570	360	−210

[a] For comparison, all values are extrapolated to 298 K. [b] Values measured in the temperature range 210−300 K. [c] Values measured in the temperature range 80−210 K; the $\Delta G°$ values at 298 K are extrapolated from the measured values of $\Delta S°$ and $\Delta H°$ at low temperature. The operating $\Delta G°$ at low temperature is much smaller (See Figure 8). [d] Difference between P* and $P^+Q_A^-$ measured by **the** photoacoustic method on the submicrosecond time scale.[21]

When the charge recombination reaction proceeds through the thermally activated route via the P^+H^- state, the $\Delta G°$ between the $P^+Q_A^-$ and P^+H^- states can be determined from the charge recombination rate at a given temperature, and the temperature dependence of the rate provides values for $\Delta H°$ and $\Delta S°$. Above about 210 K, the reaction enthalpy is found to be close to the free energy change (Figure 7). This is consistent with previous measurements on a smaller number of samples using the same method.[28,41] The entropy change is small (<3.3 meV/K) and positive, indicating that the intermediate P^+H^- state is somewhat more disordered than $P^+Q_A^-$. Between 80 and 200 K, $\Delta H°$ is much smaller, $\Delta G°$ becomes more strongly temperature dependent, and $\Delta S°$ becomes significant.

The method used here for the estimation of thermodynamic parameters of the reaction centers relies on the validity of the model illustrated in Figure 1. A few possible complications exist.

Identity of the Intermediate State. The variation of the charge recombination kinetics with the energy of the $P^+Q_A^-$ state strongly supports a mechanism whereby $P^+Q_A^-$ preequilibrates with a higher-energy intermediate (Figure 2). This intermediate is most likely P^+H^-.[2,18,23] Some controversy exists in the literature regarding the exact free energy of this state. Measurements on the nanosecond or faster time scales find

values varying from 90 to 250 meV below the free energy of P*.[43−47] Explanations for the variation include relaxation following the initial charge separation and a distribution of free energies for P^+H^-. Using 7.7×10^7 s^{-1} for k_1 and a $\Delta G°$ value between P* and $P^+Q_A^-$ of 860 meV for the native reaction centers, the thermal intermediate is 340 meV below P* in free energy. This estimate uses measurements on the micro- to millisecond time scale. The lower energy suggests the thermal intermediate state observed in $P^+Q_A^-$ charge recombination utilizes a more relaxed form of P^+H^- as the high-energy intermediate.

The free energy change from $P^+Q_A^-$ to P* has also been measured independently using the delayed fluorescence method.[18] If the free energy change of $P^+Q_A^-$ to P* is compared to the free energy change between $P^+Q_A^-$ and P^+H^-, the difference is a constant for the different quinones as Q_A (Figure 2). Thus, the free energy of the thermally accessible P^+H^- state is independent of the identity of the quinone in the Q_A binding site. Thus, regardless of the exact nature of the thermal intermediate, this state can be used as a reference point for determining the relative $P^+Q_A^-$ energy under different conditions.

Triplet Formation on the Charge Recombination Pathway. Triplet states will be formed in quinone-substituted reaction centers if the quantum yield for formation of $P^+Q_A^-$ is lower than 1. Some formation of triplet state in reaction centers containing 2-Me-AQ and 2,3-dM-AQ at low temperature is consistent with previous quantum yield measurements.[41]

The triplet state might also be formed in charge recombination via P^+H^-. Equation 1 does not account for this additional route for $P^+Q_A^-$ charge recombination. However, at low temperature, the triplet decay rate is seen to be distinct from the decay of the $P^+Q_A^-$ state, indicating that the triplet state is not in equilibrium with the P^+H^- state. It has been observed previously that no extra triplet was formed from the thermal back reaction through the P^+H^- state for 2,3-dM-AQ-substituted reaction centers.[18] Therefore, the triplet pathway seems to be separate from the thermal back-reaction route through the P^+H^- state. The observed triplet most likely arises in a subpopulation of RCs in which $P^+Q_A^-$ is never formed.

Comparison with Previous Results. The temperature dependence of $\Delta G°$, $\Delta H°$, $-T\Delta S°$ for reaction centers with 2-Me-AQ as Q_A is illustrated in Figure 8. At temperatures above 210 K, $\Delta G° \approx \Delta H°$ and $\Delta S°$ is small. At lower temperatures, $-\Delta G°$ diminishes with temperature. The interpretation presented here is a first-order approximation, which assumes $\Delta H°$ and $\Delta S°$ are constant above and below the transition temperature.

The entropy and enthalpy differences between P* and $P^+Q_A^-$ have been obtained in the room-temperature region by measuring the temperature dependence of the delayed fluorescence via the P* state. For UQ_{10}, the entropy change is 110 meV, while the free energy difference is −860 meV.[17] For AQ and 2,3,5-trimethyl-NQ, the $T\Delta S°$ values were 10 and −20 meV, respectively, relative to $\Delta G°$ values of −700 and −770 meV.[18] Thus, the reaction entropy between $P^+Q_A^-$ and P* is small.

The thermodynamic parameters of the charge separation from P* to $P^+Q_A^-$ have also been measured by a photoacoustic method, which is a more direct calorimetric measure of the enthalpy change. The results from photoacoustic measurements vary. Early estimates showed relatively small values of $\Delta S°$, in agreement with the delayed fluorescence measurement.[19,20] However, a recent study using improved methodology and submicrosecond time resolution found a surprisingly large portion of the free energy change (∼50% for UQ_{10}) to be

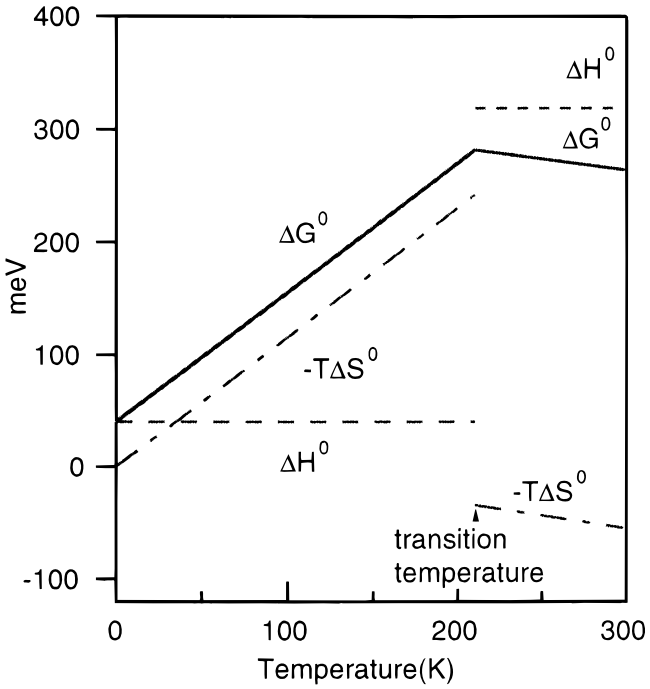

Figure 8. Temperature dependence of $\Delta G°$, $\Delta H°$, and $-T\Delta S°$ from $P^+Q_A^-$ to P^+H^- in reaction centers with 2-Me-AQ as Q_A. The region below 80 K is an extrapolation assuming constant values for $\Delta H°$ and $\Delta S°$.

entropic.[21] Possible causes of this discrepancy were discussed in detail in that paper. One important factor may be the different time scales of the measurements. It was proposed that more relaxation of $P^+Q_A^-$ occurs in the slower delayed fluorescence measurements (10 μS to 100 ms) than in the fast photoacoustic measurement (<100 ns). The thermodynamic parameters obtained here by the thermal charge recombination measurements are in good agreement with those found by delayed fluorescence. These methods both monitor the system during the lifetime of $P^+Q_A^-$.

The observation of a large entropy change at temperatures lower than 210 K also suggests that $P^+Q_A^-$ is formed in a state that can be trapped before relaxation. The reaction $\Delta S°$, if extrapolated to room temperature, is 300 mev (298 K) for 2,3-dM-AQ, which is comparable with the value of 210 meV measured by the photoacoustic method at the same temperature. At low temperature, protein motions are slowed, and the $P^+Q_A^-$ state formed by the flash may not be able to fully relax in the milliseconds before the charge recombination. A trapped state can result from energy barriers internal to the protein, as well as from high solvent viscosity.[33] The reaction entropy and enthalpy changes are, therefore, different from their values at room temperature. Thus, a large $\Delta S°$ may be found by the photoacoustic method because an early intermediate is assayed, while similar results are found below 210 K where an unrelaxed state is trapped.

Extrapolating the $-\Delta G°$ value for electron transfer with 2-Me-AQ as Q_A to 0 K show that the energy gap between $P^+Q_A^-$ and P^+H^- is 220 meV smaller than at room temperature (Figure 8). The temperature dependence of the $P^+Q_A^-$ state is likely to be greater than that of the P^+H^- state, which lives less than a nanosecond and so has little time for relaxation at any temperature. Several other, less direct, estimates of the temperature dependence of the $P^+Q_A^-$ energy level exist from estimates of the temperature dependence of the free energy gap between $P^+Q_A^-$ and the ground state. The rate of $P^+Q_A^-$ charge recombination by direct tunneling from Q_A^- to P^+ was analyzed

using a distributed-conformation model.[14] Analyzing the change in rate with quantum mechanical electron-transfer theory, the average free energy difference between $P^+Q_A^-$ and P appears to increase by about 130 meV from room temperature to 5 K. This is consistent with $P^+Q_A^-$ being trapped in a higher-energy state at low temperatures.

A similar study determined the temperature dependence of electron tunneling from Q_A^- to P^+ in mutants with different P/P^+ midpoint potentials.[34] The relationship between the electron-transfer rate and the driving force was analyzed using Marcus theory. The maximum of the theoretical curve, i.e., the driving force ($-\Delta G°$) at which the electron transfer is optimized, shifts by -280 meV from room temperature to 10 K. This shift could be explained by either a decrease of the reorganization energy (λ) or an increase in the driving force ($-\Delta G°$). The contribution of each variable could not be separated in the analysis. However, the results reported here suggest that a significant portion of the shift is due to an increase in $-\Delta G°$ as $P^+Q_A^-$ is trapped at a higher energy at low temperature.

Conclusions

The free energy, entropy, and enthalpy changes between $P^+Q_A^-$ and P^+H^- were determined for eight anthraquinones and one naphthoquinone as Q_A. The temperature dependence of the charge recombination kinetics was studied at temperatures from 40 to 318 K. The entropy changes are found to be small from 210 K to room temperature. However, in the temperature region 80−210 K, a significant entropy change is observed, and the free energy is strongly temperature dependent. Thus, at lower temperatures, $P^+Q_A^-$ appears to be trapped in a higher energy state. This is consistent with early studies that inferred changes in the energy of this state at low temperature, without being able to measure the in situ value of $\Delta G°$ directly.

Acknowledgment. We are grateful for financial support from the Department of Agriculture (CREES 1999-01256) and from NIH (RR03060) for maintenance of central facilities. We also thank Drs. David Mauzerall, Gregory Edens, and Jiali Li for helpful discussions.

References and Notes

(1) Feher, G.; Allen, J. P.; Okamura, M. Y.; Rees, D. C. *Nature* **1989**, *339*, 111.
(2) Gunner, M. R. *Curr. Top. Bioenerg.* **1991**, *16*, 319.
(3) Blankenship, R. E.; Madigan, M. T.; Bauer, C. E. *Anoxygenic Photosynthetic Bacteria*; Kluwer Academic Publishers: Dordrecht, The Netherlands, 1995; Vol. 2, p 1283.
(4) Marcus, R. A.; Sutin, N. *Biochim. Biophys. Acta* **1985**, *811*, 265.
(5) DeVault, D. *Q. Rev. Biophys.* **1980**, *13*, 387.
(6) Gopher, A.; Blatt, Y.; Schonfeld, M.; Okamura, M. Y.; Feher, G.; Montal, M. *Biophys. J.* **1985**, *48*, 311.
(7) Lin, X.; Murchison, H. A.; Nagarajan, V.; Parson, W. W.; Allen, J. P.; Williams, J. C. *Proc. Natl. Acad. Sci. U.S.A.* **1994**, *91*, 10265.
(8) Woodbury, N. W.; Allen, J. P. In *Anoxygenic Photosynthetic Bacteria*; Blankenship, R. E., Madigan, M. T., Bauer, C. E., Eds.; Kluwer Academic Publishers: Dordrecht, The Netherlands, 1995.
(9) Li, J.; Takahashi, E.; Gunner, M. R. *Biochemistry* **2000**, *39*, 7445.
(10) Kleinfeld, D.; Okamura, M. Y.; Feher, G. *Biochemistry* **1984**, *23*, 5780.
(11) Gunner, M. R.; Robertson, D. E.; Dutton, P. L. *J. Phys. Chem.* **1986**, *90*, 3783.
(12) Gunner, M. R.; Dutton, P. L. *J. Am. Chem. Soc.* **1989**, *111*, 3400.
(13) Franzen, S.; Boxer, S. G. *J. Phys. Chem.* **1993**, *97*, 6304.
(14) McMahon, B. H.; Muller, J. D.; Wraight, C. A.; Nienhaus, G. U. *Biophys. J.* **1998**, *74*, 2567.
(15) Chidsey, C. E. D.; Takiff, L.; Slodstein, R. A.; Boxer, S. G. *Proc. Natl. Acad. Sci. U.S.A.* **1985**, *82*, 6850.
(16) Polenova, T.; McDermott, A. E. *J. Phys. Chem. B* **1999**, *103*, 535.
(17) Arata, H.; Parson, W. W. *Biochim. Biophys. Acta* **1981**, *638*, 201.
(18) Woodbury, N. W.; Parson, W. W.; Gunner, M. R.; Prince, R. C.; Dutton, P. L. *Biochim. Biophys. Acta* **1986**, *851*, 6.
(19) Arata, H.; Parson, W. W. *Biochim. Biophys. Acta* **1981**, *636*, 70.
(20) Puchenkov, O. V.; Kopf, Z.; Malkin, S. *Biochim. Biophys. Acta* **1995**, *1231*, 197.
(21) Edens, G. J.; Gunner, M. R.; Xu, Q.; Mauzerall, D. *J. Am. Chem. Soc.* **2000**, *122*,1479.
(22) Gunner, M. R.; Tiede, D. M.; Prince, R. C.; Dutton, P. L. In *Function of Quinones in Energy Conserving Systems*; Trumpower, B. L., Ed.; Academic Press: New York, 1982; p 265.
(23) Shopes, R. J.; Wraight, C. A. *Biochim. Biophys. Acta* **1987**, *893*, 409.
(24) Page, C. C.; Moser, C. C.; Chen, X.; Dutton, P. L. *Nature* **1999**, *402*, 47.
(25) Takahashi, E.; Wells, T. A.; Wraight, C. A. In *Proceedings of the XIth International Photosynthesis Congress*; Garab, G., Ed.; Kluwer Academic Publishers: Dordrecht, The Netherlands, 1998; Vol. II; p 17.
(26) Warncke, K.; Dutton, P. L. *Biochemistry* **1993**, *32*, 4769.
(27) Kleinfeld, D.; Okamura, M. Y.; Feher, G. *Biophys. J.* **1985**, *48*, 849.
(28) Sebban, P. *Biochim. Biophys. Acta* **1988**, *936*, 124.
(29) Kakitani, T.; Kanitani, H. *Biochim. Biophys. Acta* **1981**, *635*, 498.
(30) Sebban, P.; Wraight, C. A. *Biochim. Biophys. Acta* **1989**, *974*, 54.
(31) Vitcup, D.; Ringe, D.; Petsko, G. A.; Karplus, M. *Nat. Struct. Biol.* **2000**, *7*, 34.
(32) Daniel, R. M.; Smith, J. C.; Ferrand, M.; Héry, S.; Dunn, R.; Finney, J. L. *Biophys. J.* **1998**, *75*, 2504.
(33) Hagen, S. J.; Hofrichter, J.; Eaton, W. A. *Science* **1995**, *269*, 959.
(34) Ortega, J. M.; Mathis, P.; Williams, J. C.; Allen, J. P. *Biochemistry* **1996**, *35*, 3354.
(35) Clayton, R. K.; Wang, R. T. *Methods Enzymol.* **1971**, *23*, 696.
(36) Okamura, M. Y.; Isaacson, R. A.; Feher, G. *Proc. Natl. Acad. Sci. U.S.A.* **1975**, *72*, 3492.
(37) Chidsey, C. E. D.; Kirmaier, C.; Holten, D.; Boxer, S. G. *Biochim. Biophys. Acta* **1984**, *766*, 424.
(38) Franzen, S.; Goldstein, R. F.; Boxer, S. G. *J. Phys. Chem.* **1990**, *94*, 5135.
(39) Lavalette, D.; Tetreau, C.; Brochon, J.; Livesey, A. *Eur. J. Biochem.* **1991**, *196*, 591.
(40) Schenck, C. C.; Blankenship, R. E.; Parson, W. W. *Biochim. Biophys. Acta* **1982**, *680*, 44.
(41) Gunner, M. R. Ph.D. Thesis, University of Pennsylvania, Philadelphia, PA, 1988.
(42) Norris, J. R.; Bowman, M. K.; Budil, D. E.; Tang, J.; Wraight, C. A.; Closs, G. L. *Proc. Natl. Acad. Sci. U.S.A.* **1982**, *79*, 5532.
(43) Holzwarth, A. R.; Muller, M. G. *Biochemistry* **1996**, *35*, 11820.
(44) Woodbury, N. W. T.; Parson, W. W. *Biochim. Biophys. Acta* **1984**, *767*, 345.
(45) Goldstein, R. A.; Takiff, L.; Boxer, S. G. *Biochim. Biophys. Acta* **1988**, *934*, 253.
(46) Ogrodnik, A.; Volk, M.; Michel-Beyerle, M. E. *Biochim. Biophys. Acta* **1988**, *936*, 361.
(47) Ogronik, A.; Keupp, W.; Volk, M.; Aumeier, G.; Michele-Beyerle, M. E. *J. Phys. Chem.* **1994**, *98*, 3432.